ELSEVIER

Journal of Molecular Structure 509 (1999) 221–236

Journal of
MOLECULAR
STRUCTURE

www.elsevier.nl/locate/molstruc

Conformational properties of bis(difluoromethyl) ether as studied by microwave, infrared, Raman spectroscopy and by ab initio computations ☆

A. Horn, K.-M. Marstokk, H. Møllendal, C.J. Nielsen*, D.L. Powell[1]

Department of Chemistry, The University of Oslo, PO Box 1033 Blindern, N-0315 Oslo, Norway

Received 17 March 1999; accepted 6 April 1999

Abstract

Bis(difluoromethyl) ether, $CHF_2–O–CHF_2$ (E134), was studied by microwave, infrared and Raman spectroscopy and by quantum chemical methods. Ab initio calculations show the existence of three conformations with H–C–O–C–H arranged *antiperiplanar–synperiplanar* (AS), *antiperiplanar–antiperiplanar* (AA) and *synclinal–synclinal* (*gauche–gauche*, GG), with relative enthalpies of ca. 0, 8 and 4 kJ mol^{-1}, respectively. Infrared spectra of the vapour and of the amorphous solid and crystalline state were obtained between 4000 and 10 cm^{-1}. The spectra of the compound isolated in argon and nitrogen matrices at 5 K were also recorded. Raman spectra of the cooled liquid and of the amorphous and crystalline solids were obtained in the region 4000–20 cm^{-1}. Two conformers with an estimated enthalpy difference of 7 ± 2 kJ mol^{-1} were detected in the liquid phase. The matrix isolation spectra also suggest the existence of more than one conformer in the vapour phase. The vibrational spectra were assigned with the aid of normal coordinate calculations employing harmonic force fields from the ab initio study. The microwave spectrum was investigated in the 10.0–38.0 GHz spectral region at 195 K. One conformer, *antiperiplanar–synperiplanar* with one H–C–O–C dihedral angle of 177° and the other 12° from *syn*, was assigned. The ground state spectrum is accompanied by a series of strong lines from the vibrational excited states; of these, five states of the ν_{21} torsional mode were assigned and analysed in terms of a double minimum potential with a barrier of 19 cm^{-1} in the *syn* position.

Keywords: Ab initio calculations; Conformations; Vibrational spectra; Fluoroethers

1. Introduction

As it has become more important to find replacement compounds for the various freons which have been outlawed, those compounds which might be suitable candidates as substitutes have been the subject of numerous investigations. The title compound, bis(difluoromethyl) ether—E134, is no exception to this. At least as far back as 1990 when a variety of possible fluorinated compounds were being considered, it was placed in a class of compounds, which warranted further study for this purpose [1].

Since that time, it has been included in a variety of studies. Its dipole moment in the gas phase was determined and found to vary with temperature, which was interpreted as an evidence that the compound contained more than one conformer [2].

☆ Dedicated to Professor Peter Klæboe on the occasion of his 70th birthday.

* Corresponding author. Tel.: + 47-22-855446; fax: + 47-22-855441.

E-mail address: claus.nielsen@kjemi.uio.on (C.J. Nielsen)

[1] On leave from the College of Wooster, Wooster, Ohio, USA.

0022-2860/99/$ - see front matter
PII: S0022-2860(99)00223-9

Various physical properties of the vapour [3,4] and of the vapour and liquid [5] have been measured.

The title compound is a member of an interesting class, not just as potential refrigerants, but as inhalation anaesthetics. In this connection, its rotational barriers were calculated using ab initio methods along with those of a total of nine other fluorinated dimethyl ethers [6].

Some earlier spectroscopic work has recently appeared. This includes a microwave spectroscopic structure determination [7], and the infrared absorption cross-section [8–10]. In connection with the work on surfaces, its infrared spectrum was recorded and some assignments made [11]. Its spectrum was also recorded in a matrix in a study of its hydrogen bonding interaction with several bases [12]. However, in none of these cases, was it studied thoroughly in its own right. Work on atmospheric lifetimes, infrared spectra and the degradation products of several hydrofluoropolyethers has been done [13], as has further work on the vibrational spectra and quantum chemical calculations of some polyfluoroethers [14].

Less directly relevant to this study are kinetics measurements involving the title compound. For example, several groups [15–17] have reported data on its reaction with the hydroxyl radical.

2. Experimental

The sample of bis(difluoromethyl) ether, obtained from Ausimont S.p.A., had a stated purity of more than 98%, and was used without further purification after degassing and distillation in vacuo; no disturbing impurities were observed. The MW spectrum was studied using the Oslo Stark spectrometer, which is described in Ref. [18]. The 10–38 GHz spectral region was investigated with the microwave absorption cell cooled to dry-ice temperature (195 K). The spectra were recorded at a pressure of about 5 Pa and stored electronically using the computer programs written by Waal [19]. The accuracy of the frequency measurements is presumed to be better than ± 0.10 MHz.

Infrared spectra of the sample in the vapour and as crystalline solids were recorded using a Bruker Model 113v and a Perkin–Elmer Model 2000 FTIR, employing conventional cells and LN2 cooled cryostats. The spectrum of the matrix-isolated compound was recorded with a Bruker Model 88 using a closed-cycle helium cooled Displex unit from APD (model HS-4) with windows of CsI. The compound was mixed with argon or nitrogen in the ratio 1:1000 and the gas mixtures were deposited on the cold window at ca. 5 K. After the unannealed samples had been recorded at 5 K, the samples were first annealed at 20 K and later at 34 (argon), 32 K (nitrogen), before the spectra of the annealed samples were recorded.

Raman spectra of the liquid, amorphous solid and crystalline states were recorded using a Dilor RTI-30 spectrometer (triple monochromator) using the 514.5 nm line from a Spectra Physics model 2000 argon ion laser for excitation. The liquid spectra were obtained of an ampoule inserted in a Dewar [20], and cooled with gaseous nitrogen evaporating from a reservoir equipped with a heating element. Solid samples were produced by depositing the vapour onto a copper block in the LN2 cooled Raman cryostats.

3. Results and discussion

3.1. Quantum chemical calculations

The GAUSSIAN 94 program package [21] running on

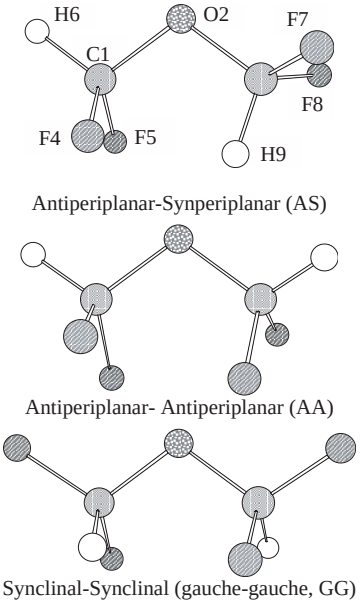

Fig. 1. The three conformations of bis(difluoromethyl) ether, E134.

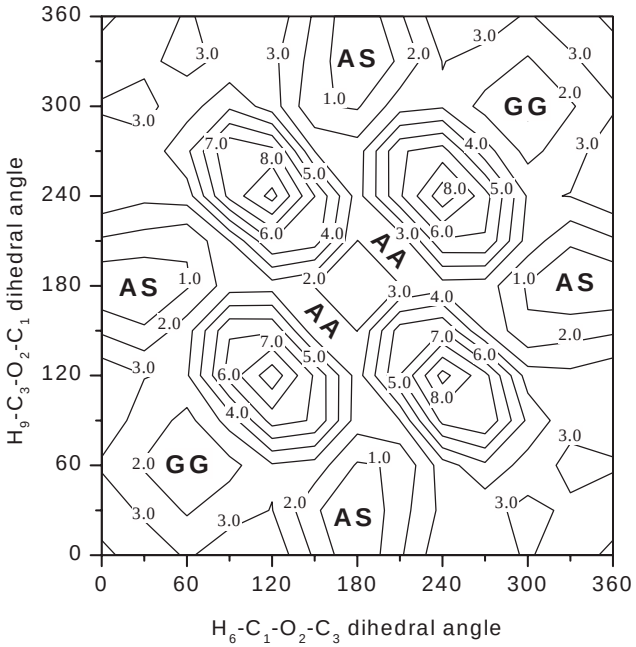

Fig. 2. The potential energy surface/kcal mol^{-1} of bis(difluoromethyl) ether, E134, calculated on the RHF level employing the 6-31G* basis set. Data taken from Ref. [5]. The potential energy minima have been labelled AA (antiperiplanar–antiperiplanar), AS (antiperiplanar–synperiplanar), and GG (synclinal–synclinal, gauche–gauche).

the IBM RS6000 cluster in Oslo was employed in the quantum chemical calculations. The conformational properties of E134 are determined by two dihedral angles, e.g. the H6–C1–O2–C3 and H9–C3–O2–C1 dihedral angles (see Fig. 1). The torsional potential surface was previously mapped by varying these two angles systematically in steps of 30°, and calculating the energy at the Hartree–Fock level employing the 6-31G* basis set [5]. Fig. 2 shows a contour plot of their data. Inclusion of electron correlation at the MP2/6-31G**//6-31G** level was reported to have little effect on the relative energy of the conformers. As can be seen, three minima are predicted and the corresponding rotamers *antiperiplanar–synperiplanar* (AS), *antiperiplanar–antiperiplanar* (AA) and *synclinal–synclinal* (*gauche–gauche*, GG) are drawn in Fig. 1. AS has C_1 symmetry while AA and GG both have C_2 symmetry. The statistical weight of AS is four, whereas the statistical weight of the other two rotamers is two in each case.

Elaborate MP2/6-311++G** computations with full optimisation of structures were then made for these three rotamers using the 6-31G* structures as starting points. Electron correlation is included in this computational scheme using the second order Møller–Plesset (MP2) perturbation theory [22], with frozen-core electrons [21]. This computational procedure was chosen because it is our experience [23] that the structure (and rotational constants) are rather accurately predicted in the computations at the MP2/6-311++G** level. Indeed, the rotational constants of the AS rotamer, which is the only conformer that has been assigned [7], were computed (Table 1) to be within 1% of the observed values [7] (see later). Another reason for choosing this computational scheme is that the energy differences between the conformers are normally well reproduced. The optimised geometries, zero-point corrected energy differences, dipole moments and calculated rotational constants are listed in Table 1. Suenram et al. [7], employing a "double zeta" basis set, predicted a fourth *synclinal–synclinal* (*gauche–gauche$'$*, GG$'$) conformer of the C_s symmetry with torsional angles of ca. 60 and $-60°$, and with still higher energy than AA. Using the larger 311++G** basis set we found that this conformation corresponds to a saddle point.

Table 1
Structure, rotational constants, dipole moment and energy differences of the three stable rotamers of E134 as calculated at the MP2/6-311++G** (frozen core) level of theory. Atom numbering is given in Fig. 1

Conformer	*Antiperiplanar–synperiplanar*		*Antiperiplanar–antiperiplanar*		*Synclinal–synclinal*	
Distance (pm)						
C1–O2	136.8		138.3		138.0	
O2–C3	138.8		138.3		138.0	
C1–F4	135.8		134.7		133.4	
C1–F5	135.5		135.0		136.0	
C1–H6	108.6		108.7		108.9	
C3–F7	134.2		134.7		133.4	
C3–F8	134.6		135.0		136.0	
C3–H9	108.8		108.7		108.9	
Angle (°)						
C1–O2–C3	115.8		119.6		114.9	
O2–C1–F4	111.0		111.9		106.3	
O2–C1–F5	111.2		110.8		110.0	
O2–C1–H6	108.3		107.1		113.4	
O2–C3–F7	107.3		111.9		106.3	
O2–C3–F8	108.8		110.8		110.0	
O2–C3–H9	113.3		107.1		113.4	
Dihedral angle (°)						
C3–O2–C1–F4	61.7[a]		40.9		−179.1	
C3–O2–C1–F5	−56.4		−79.0		−62.0	
C3–O2–C1–H6	−177.6		161.8		59.5	
C1–O2–C3–F7	−134.0		40.9		−179.1	
C1–O2–C3–F8	109.6		−79.0		−62.0	
C1–O2–C3–H9	−12.4		161.8		59.5	
Rotational constants (MHz)						
A	4590.5		4357.1		5214.4	
B	1914.6		2197.6		1570.6	
C	1522.2		1937.0		1476.3	
Dipole moment components[b] and total dipole moment (10^{-30} C m)						
	MP2	B3LYP	MP2	B3LYP	MP2	B3LYP
μ_a	5.92	5.04	0.0	0.0	0.0	0.0
μ_b	0.91	1.10	0.0	0.0	0.0	0.0
μ_c	0.50	0.43	8.61	5.87	6.27	7.98
μ_{tot}	6.01	5.17	8.61	5.87	6.27	
Energy difference (kJ mol^{-1})[c]						
	0.0[d]		8.7		3.8	

[a] Measured from syn = 0°. Clockwise rotation correspond to positive dihedral angle.
[b] Along the principal inertial axes.
[c] Relative to antiperiplanar–synperiplanar.
[d] Total energy obtained in the MP2 computations: −1 328 460.75 kJ mol^{-1}.

Some of the results presented in this table deserve comment: it is seen that AS is predicted to be the most stable rotamer. It is computed to be 8.7 kJ mol^{-1} more stable than AA and 3.8 kJ mol^{-1} more stable than GG. The fact that AS is clearly the preferred form of the molecule is in agreement with the experimental results presented below.

There is nothing unusual about the bond lengths and bond angles of any of the three conformers. However, while the conformation of the GG rotamer is computed to be rather normal with dihedral angles close to the expected ± 60 or 180°, unusual conformations are seen for the two other rotamers: AA is remarkable in that the CHF_2 groups are twisted approximately 20° from their usual position.

The conformation of AS is, in our opinion, extraordinary. This rotamer is predicted to have a very unusual structure in that the C3–H9 bond nearly eclipses the C1–O2 bond. The C1–O2–C3–H9 dihedral angle is calculated to be about 12° (!) from being completely *syn*. The authors know no other similar example. The H6–C1–O1–C2 dihedral angle has, however, a normal anti-value of approximately 180° (Table 1).

There is no straightforward explanation why E134 takes the remarkable AS conformation as its preferred form. Perhaps non-bonded interactions between the highly electronegative fluorine and oxygen atoms are a major effect in this case.

A value of 0° for the C1–O2–C3–H9 dihedral angle for symmetry reasons must be a maximum on the potential energy surface. Additional computations at the same level of theory (MP2/6-311++G^{**} with frozen core electrons) confirmed this assumption. The barrier height was computed to be only 0.036 kJ mol^{-1} (3 cm^{-1}). One negative vibrational frequency (-17 cm^{1}), identified to be the O2–C3 torsional frequency, was calculated in this case.

Density functional theory computations are known to yield rather accurate results for dipole moments and vibrational frequencies. The computations of the harmonic force field employing the B3LYP functional [24] and the 6-311++G^{**} basis set were also made. The ab initio cartesian force fields (B3LYP) were subsequently transformed into symmetry force fields corresponding to a suitable set of internal coordinates.

3.2. Vibrational spectra and assignment

The infrared and Raman spectral data is collected in Table 2. The bands obviously due to site effects in the matrix spectra, and which disappear upon annealing to 20 K are not included in the table. Infrared vapour-phase spectra of E134 are shown in Fig. 3 (4000–400 cm^{-1}) and Fig. 4 (600–10 cm^{-1}), while Fig. 5 shows a Raman spectrum (1600–100 cm^{-1}) of the liquid at −10°C.

The vapour phase IR band contours were calculated for the three conformers of E134 by adding rotational transitions for $J = 0$–100 without taking a centrifugal distortion into consideration, and assuming a spectral resolution of 1 cm^{-1} (adding a centrifugal distortion will result in substantially broader Q-branches). There is very little difference in the contours of the three conformers and only the results for the AS conformer are shown in Fig. 6; the PR-separation is ca. 13, 8 and 16 cm^{-1} for the A-, B- and C-type bands, respectively. Figs. 3 and 4 show the IR spectrum contains a number of bands with distinct vapour contours. However, only the C–H stretching bands, Fig. 7, are sufficiently of a characteristic shape to give an indication to the preferred conformation in the vapour. The position of the principal axis is such that the two C–H stretching bands should both show *C*-type contours for the AS conformer. For the AA conformer, they should be of (A)/B- and C-type, respectively, while they should be of *A*/(*B*)- and C-type for the GG form. As can be seen from Figs. 6 and 7, both the bands are clearly of C-type suggesting that the AS conformer is the dominating form in the vapour.

There are no dramatic differences between the liquid-phase spectra obtained at different temperatures, the spectra of the amorphous solid, and those of the crystal. In fact, only two bands change their intensity significantly with decreasing temperature. The conclusion to be drawn is that one conformer, the AS (see later), dominates all the states of aggregation.

The 367 cm^{-1} band seen in the liquid phase Raman spectrum decreases in intensity as the liquid is cooled, and is not at all present in the crystal phase. At the same time the band at 585 cm^{-1}, which is essentially not present at room temperature, increases during cooling. Apart from these, the only changes are the disappearance of shoulders at 794 cm^{-1} on the band at

Table 2
Infrared and Raman spectral data for bis(difluoromethyl) ether, E134 (weak infrared bands in the region 2900–1500 cm^{-1} have been omitted; s, strong; m, medium; w, weak; v, very; br, broad; sh, shoulder; Q, Q-branch)

Infrared				Raman		Interpretation
Vapour	N_2 matrix (5 K)	Ar Matrix (5 K)	Crystal (77 K)	Liquid (270 K)	Crystal (77 K)	
3058m,C	3076w	3061w	3080w	3062w	3091m	ν_1
3052m,C	3068w				3079m	
3044m,C						
		3051vw[a]				AA
3039m,C	3048w	3030w	3064vw	3041w	3062mw	ν_2
3032m,C	3043w		3058vw		3056mv	
3023m,C						
3014w,sh		3012vw[a]				GG
			1420vw,sh			
1416m,Q	1417m	1415m	1419m	1420vw	1418w	ν_3
1393m	1390m	1390m	1391m	1390w	1393mw	ν_4
					1387mw	
1385s						
1379s		1382w[a]				AA/GG
		1379w[a]				
1373s			1368vw			
1365s			1359m,sh			
1360s	1364m	1358m	1356m	1365w	1358mw	ν_5
	1360m					
1355s			1352w,sh			
1349m	1353m	1348m	1346mw	1355vw,sh	1349w	ν_6
	1349m					
			1343w,sh			
	1287vw	1289vw				
1273vw		1267vw				
1238vw,Q	1237w		1237w			
		1202m[a]				GG
1201m	1194s	1197m	1196m,sh	1202w	1188vw	ν_7
			1190m			
1199mw	1180w	1184w				
		1174w				
1165s,sh	1161m	1161w	1162m,sh			
		1151vs[a]	1150s		1152vvw	AA/GG
1140vs,br	1145vs	1146vs	1138s	1040w,sh	1136mw	ν_8
	1126vs	1127vs	1120vs	1126m,br	1111vw,sh	ν_9
	1120vs	1116m	1112s		1106mw	
			1090s,sh			
	1093m	1083w	1080vs	1090mw,sh	1082mw	ν_{10}
1090m,B	1075s	1077s	1062s,sh	1071mw,br	1055mw	ν_{11}
1081m,B	1072s		1053s			
		1069m[a]				
	1057w	1061w				
		1010w,sh				
1015m,A	1002s	1008m	1002ms	1009s	1003ms	ν_{12}
1009m,A	1001		996s		995s	
1003m,A						
		1004s				
		1000vw				
	992vw	996vw				

Table 2 (*continued*)

Infrared				Raman		Interpretation
Vapour	N_2 matrix (5 K)	Ar Matrix (5 K)	Crystal (77 K)	Liquid (270 K)	Crystal (77 K)	
	982vw	987vw	985w			
913vw				913vw		
869vw						
				794vw,sh		AA/GG
791m,A	783m	783s	780s	785mw	780m	ν_{13}
785m,A	781m		778m,sh			
779m,A						
			773w,sh			
			772W,sh			
761vw,sh	767m	767m[a]		765vvw		AA/GG
				748vvw		
				694vvw		
			638w	638ms	635m	ν_{14}
					628mw	
584vw,B	580w	580w	581w	585w,br	583w	ν_{15}
574vw,B						
537mw,A	530m	531m	531m	532w	531w	ν_{16}
531mw,A						
525mw,A						
				523vvw		A/GG
			458w,sh		457vw,sh	
458w,A	455w	458w	454m	453mw	452w	ν_{17}
452w,A						
446w,A						
				399mw	403ms	ν_{18}
				393w,sh		AA/GG
				369m	[a]	AA/GG
215vw			221w	218m	221mw	ν_{19}
			117w		115vw	Lattice
84vw			80vw	∽ 75w	79w	ν_{20}
34vw			42vw		50w	ν_{21}

[a] Band disappears upon annealing; *A*, *B* and *C* denote infrared vapour-phase contours; AA, *antiperiplanar–antiperiplanar* conformer; GG, *synclinal–synclinal* (*gauche–gauche*) conformer.

785 cm^{-1} and at 393 cm^{-1} on the band at 398 cm^{-1}. Although the evidence for conformational equilibria in the liquid phase is not overwhelming, it is indisputable and an analysis of the intensity variation of 369 cm^{-1} versus the 399, 453 and 785 cm^{-1} bands with temperature (van't Hoff plot) suggests a conformational enthalpy difference of 7 ± 2 kJ mol^{-1} in the liquid.

Two crystal forms containing the same conformer were observed. For the sake of brevity, only the spectral data for the most stable form is given in Table 2. When the sample was deposited on the window in their cryostat, it was already crystalline (crystal I). It changed to a slightly different crystal (crystal II) when annealed to ca. 100 K. The sample was lost when the window was allowed to warm to ca. 125 K. The sample, which was deposited on the copper block in the Raman cryostat, was amorphous. It converted to crystal I when annealed to ca. 90 K and to crystal II when annealed to a slightly higher temperature. The most interesting aspect about the crystal phases was observed in the C–H stretching region. In crystal I, there are just two peaks (in both infrared and Raman—they coincide) which correspond to the two C–H linkages which are oriented differently and thus have different C–H stretching frequencies. In crystal II, there are three peaks in this region in the infrared and four in the Raman. The three active peaks

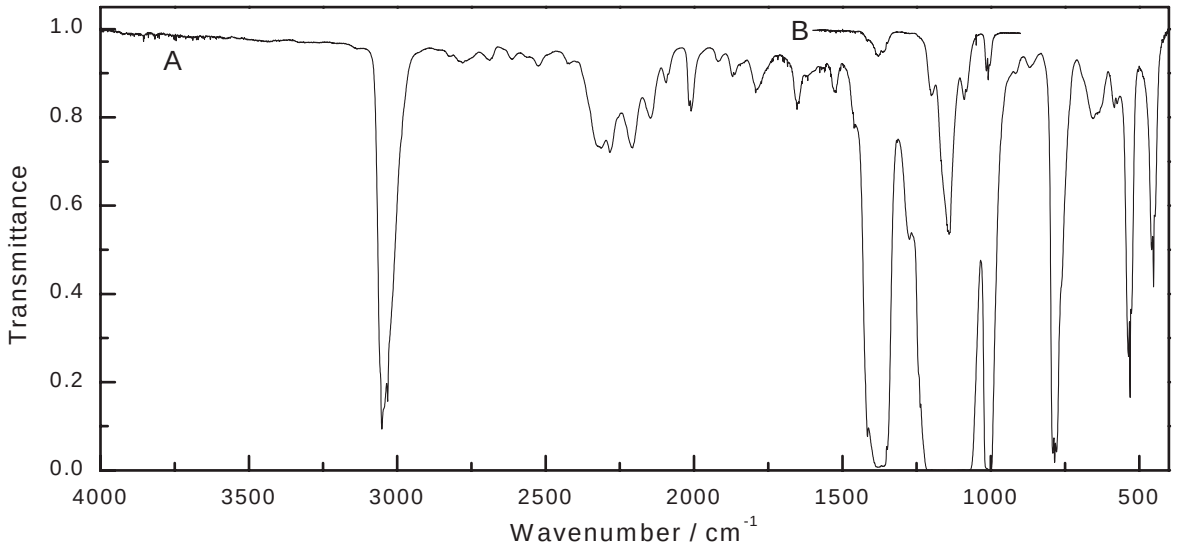

Fig. 3. The IR spectrum (4000–400 cm^{-1}) of bis(difluoromethyl) ether, E134, as a vapour. Path length 10 cm; spectral resolution 0.5 cm^{-1}; A, 80; B, 0.8 hPa.

in both effects coincide with each other. Our interpretation is that in the more stable crystal there are two molecules in the unit cell and that the environment, which the hydrogen experience, are somewhat different. This leads to different C–H stretching frequencies, but very little change in the frequencies for the rest of the molecule.

The argon matrix spectra also show indications of more than one conformer being present in the vapour phase. A number of distinct bands are present in the argon spectra but not in the nitrogen spectra. The same bands disappear upon annealing to 34 K and have been marked by asterisks in Table 2, and are attributed to the AA or GG conformers; we have no experimental criteria to be more specific.

With the aid of the normal coordinate calculations, the vibrational assignment of the most stable conformer was made rather easily. The calculated wavenumbers at the B3LYP/6-311++G^{**} level only need a 2–3% scaling to fit the observations. The scaling procedure we advocate is to (i) transform the ab initio force fields from Cartesian co-ordinates to a set of suitable internal co-ordinates and (ii) scale these according to the types of internal co-ordinates using the scheme: $F_{ij}(\text{scaled}) = F_{ij}(\text{ab initio})\cdot(x_i\cdot x_j)^{1/2}$, where x_i and x_j are scale factors for the diagonal force constants corresponding to internal co-ordinates i and j, respectively [25]. A set of scale factors, common to all conformers, is then applied to classes of internal co-ordinates of the same type (in the present case there are nine different valence co-ordinates).

The calculations are summarised in Table 3 with an approximate description of the fundamental modes. They clearly show the different surroundings of the two H-atoms: the ca. 20 cm^{-1} separation between the two C–H stretching frequencies, that there is little

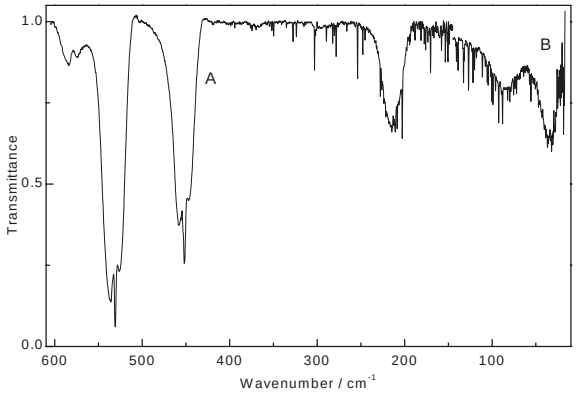

Fig. 4. The IR spectrum (600–10 cm^{-1}) of bis(difluoromethyl) ether, E134, as a vapour. Path length, 19 cm; spectral resolution 0.5 cm^{-1}; pressure, 71 hPa; A, 3.5 μ; B, 12 μ beamsplitter.

Table 3
Observed and calculated fundamentals/cm^{-1} for the three conformers of bis(difluoromethyl) ether, E134

Antiperiplanar–synperiplanar (AS)				*Antiperiplanar–antiperiplanar* (AA)			*Synclinal–synclinal* (*gauche–gauche*, GG)	
Mode	Observed	Calculated	Approximate description	Calculated		Observed		Calculated
ν_1	3052	3057	CH_a stretch[a]	3040 (a)	3051[b]			3013 (a)
ν_2	3032	3027	CH_s stretch[a]	3036 (b)			3014	3009 (b)
ν_3	1416	1419	Sym. OCH bend	1423 (a)				1416 (a)
ν_4	1393	1391	Antisym. OCH bend	1381 (b)		1382[b]		1382 (a)
ν_5	1360	1360	FCH bend	1366 (a)		1379[b]		1379 (b)
ν_6	1349	1348	FCH bend	1361 (b)				1353 (b)
ν_7	1201	1204	Antisym CO stretch	1171 (b)			1202[b]	1209 (a)
ν_8	1140	1150	CF_2 stretch	1169 (a)		1151[b]		1151 (b)
ν_9	1126[c]	1125	CF_2 stretch	1119 (b)				1142 (b)
ν_{10}	1090	1121	CF_2 stretch	1080 (a)				1117 (a)
ν_{11}	1085	1060	CF_2 stretch	1044 (b)		1069[b]		1056 (a)
ν_{12}	1009	993	Sym. CO stretch	1037 (a)				1045 (b)
ν_{13}	785	791	OCF_2 wag	789 (a)		794[c], 767[b]		780 (b)
ν_{14}	638[c]	629	Sym. FCF bend	647 (b)				608 (a)
ν_{15}	579	585	OCF_2 twist	572 (b)				581 (a)
ν_{16}	531	529	Antisym. FCF bend	529 (a)		523[b]		529 (b)
ν_{17}	452	455	OCF_2 wag	473 (b)				482 (b)
ν_{18}	399[c]	403	OCF_2 twist	382 (a)		393[b], 369[b]		363 (a)
ν_{19}	215	212	COC bend	186 (a)				190 (a)
ν_{20}	84	86	$-CF_2H_a$ torsion	123 (b)				93 (b)
ν_{21}	34	30	$-CF_2H_s$ torsion	47 (a)				55 (a)

[a] Subscripts “a” and “s” denote the antiperiplanar and synperiplanar hydrogens, respectively, in the AS conformer, see Fig. 1.
[b] Argon matrix data.
[c] Liquid phase Raman data.

mixing between these frequencies, and that each is essentially associated with the motion of just one of the two hydrogen atoms. The next four frequencies are associated with the C–H bends. The antisymmetric and symmetric C–O stretching modes at 1201 and 1009 cm^{-1} are separated by a wealth of strong, broad and overlapping IR bands from 1150 to 1050 cm^{-1}, accompanied by medium to weak bands in the Raman effect. All the heavy atom bending modes fall exactly as predicted by the

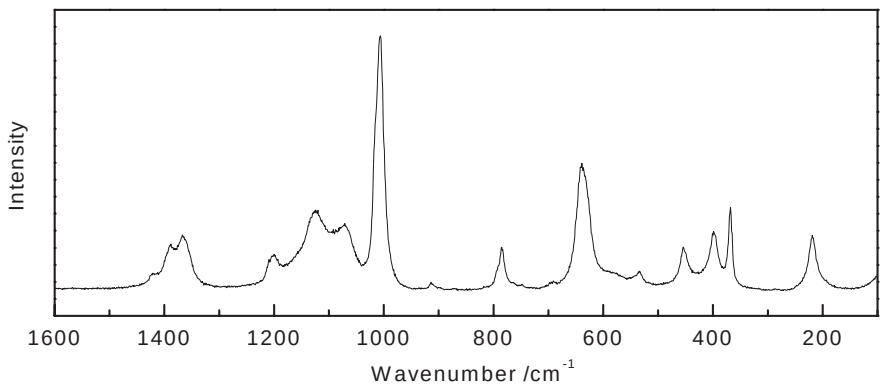

Fig. 5. The Raman spectrum (1600–100 cm^{-1}) of bis(difluoromethyl) ether, E134, as a liquid at 263 K.

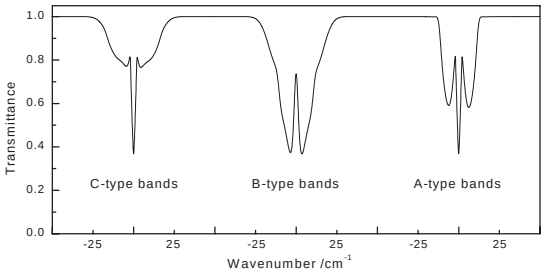

Fig. 6. The calculated IR vapour contours for bis(difluoromethyl) ether, E134.

calculations, the lowest one being the COC deformation. As is the case for the CH stretching modes, the two torsional fundamentals are almost completely local: the *antiperiplanar* group (C1F4F5H6 in Fig. 1) is associated with the band at 84 cm^{-1}, the *synperiplanar* group is associated with the 34 cm^{-1} band.

The bands and shoulders that disappear upon annealing can be explained by AA and/or GG modes. A tentative assignment of these bands is included in Table 3.

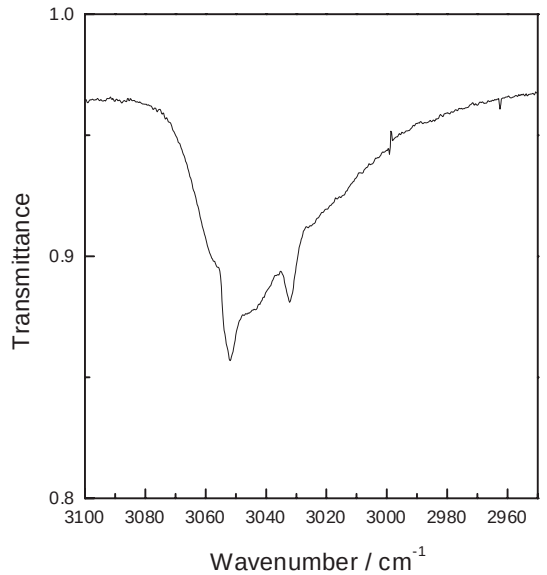

Fig. 7. The IR spectrum of E134 in the C–H stretching region (3100–2950 cm^{-1}). Path length 10 cm; spectral resolution 0.5 cm^{-1}; pressure 40 hPa.

3.3. Microwave spectrum and vibrationally excited states of antiperiplanar–synperiplanar

The MW spectrum of E134 is dominated by the a-type R-branch transitions, whose ground vibrational state transitions have already been assigned by Suenram et al. [7], who kindly made their spectroscopic constants available to us prior to publication. These constants facilitated a straightforward assignment of 78 ^{a}R transitions of the ground vibrational state. ^{a}Q transitions were not found, presumably because they are too weak. Attempts to find b- and c-type lines failed, because they have too low intensities owing to small μ_b and μ_c dipole moment components (see Section 3.5). The transitions were fitted using Watson's A-reduction I^r representation [25] for the spectroscopic constants. Significant values were obtained only for two quartic centrifugal distortion constants, viz. Δ_J and Δ_{JK}. The three remaining quartic constants were constrained to zero in the final fit. The results are shown in Table 4[2].

Suenram et al. [7] performed their experiment in a pulsed nozzle Fourier transform spectrometer which allows observation of rotational transitions at an effective rotational temperature of a few kelvin. The present wave-guide study is made at an equilibrium temperature of 195 K. Our experiment made it possible to observe several series of transitions presumably belonging to vibrationally excited states. These states form a complicated pattern as illustrated for the $6_{1,6} \leftarrow 5_{1,5}$ transition shown in Fig. 8. Nine vibrational excited states belonging to three different normal vibrational modes were ultimately assigned; their spectroscopic constants are included in Table 4.

The most intense excited state, denoted as $\nu_{21} = 1$ in Fig. 8, has about 90% of the intensity of the ground vibrational state at 195 K. Its energy was determined to be 15(10) cm^{-1} by relative intensity measurements made largely as described in Ref. [27]. Several selected rotational transitions were used to derive this value. This is close to 21 cm^{-1} predicted by the MP2 computations and 29 cm^{-1} in the B3LYP calculations for the torsion around the O2–C3 bond.

[2] The spectra of the ground and the vibrationally excited states are available from the authors upon request, or from the Molecular Spectra Data Center, National Institute of Science and Technology, Optical Technology Division, Bldg. 221, Rm. B208, Gaithersburg, MD 20899, USA, where they nhave been deposited.

Table 4
Spectroscopic constants (*A*-reduction, I^r-representation [26]; uncertainties represent one standard deviation) of the ground state and vibrational excited states of the antiperiplanar–synperiplanar rotamer of E134

Vibrational state	Ground state	$\nu_{21}=1$	$\nu_{21}=2$	$\nu_{21}=3$	$\nu_{21}=4$	$\nu_{21}=5$	$\nu_{20}=1$	$\nu_{20}=2$	$\nu_{19}=1$	$\nu_{comb.}$
No. of transitions	78.0	72.0	83.0	68.0	66.0	46.0	62.0	62.0	74.0	26.0
R.m.s. dev. (MHz)[a]	0.102	0.087	0.092	0.087	0.092	0.101	0.094	0.085	0.090	0.101
Energy (cm^{-1})[b]	0.0	15.0(10)	27.0(10)	60.0(15)	88.0(20)	160.0(25)	83.0(20)	ca.200	ca.150	ca.200
A_n (MHz)	4631.15(12)	4648.278(94)	4649.96(12)	4661.05(10)	4669.29(11)	4682.99(12)	4657.52(12)	4660.21(11)	4642.90(10)	4672.64(21)
B_n (MHz)	1912.991 6(37)	1914.368 3(29)	1911.978 6(32)	1910.574 5(31)	1909.149 7(36)	1906.899 0(36)	1913.114 1(34)	1909.305 0(32)	1912.260 3(32)	1907.361 8(51)
C_n (MHz)	1524.127 7(38)	1529.220 8(33)	1530.031 1(35)	1533.693 1(34)	1536.244 5(37)	1539.789 2(44)	1526.340 2(37)	1528.420 6(37)	1521.678 4(33)	1537.130 7(60)
Δ_J (kHz)	0.370(16)	0.142(13)	0.215(50)	0.220(13)	0.220(15)	0.285(19)	0.169(14)	0.193(14)	0.350(14)	0.405(26)
Δ_{JK} (kHz)[c]	38.451(43)	−23.035(47)	6.941(31)	5.483(31)	10.250(44)	4.181(73)	−16.205(34)	6.432(28)	25.325(33)	−18.26(11)

[a] Root-mean-square deviation.
[b] Relative to the ground vibrational stsate.
[c] Other quartic constants (δ_J,δ_K and δ_{JK}) constrained to zero; see text.

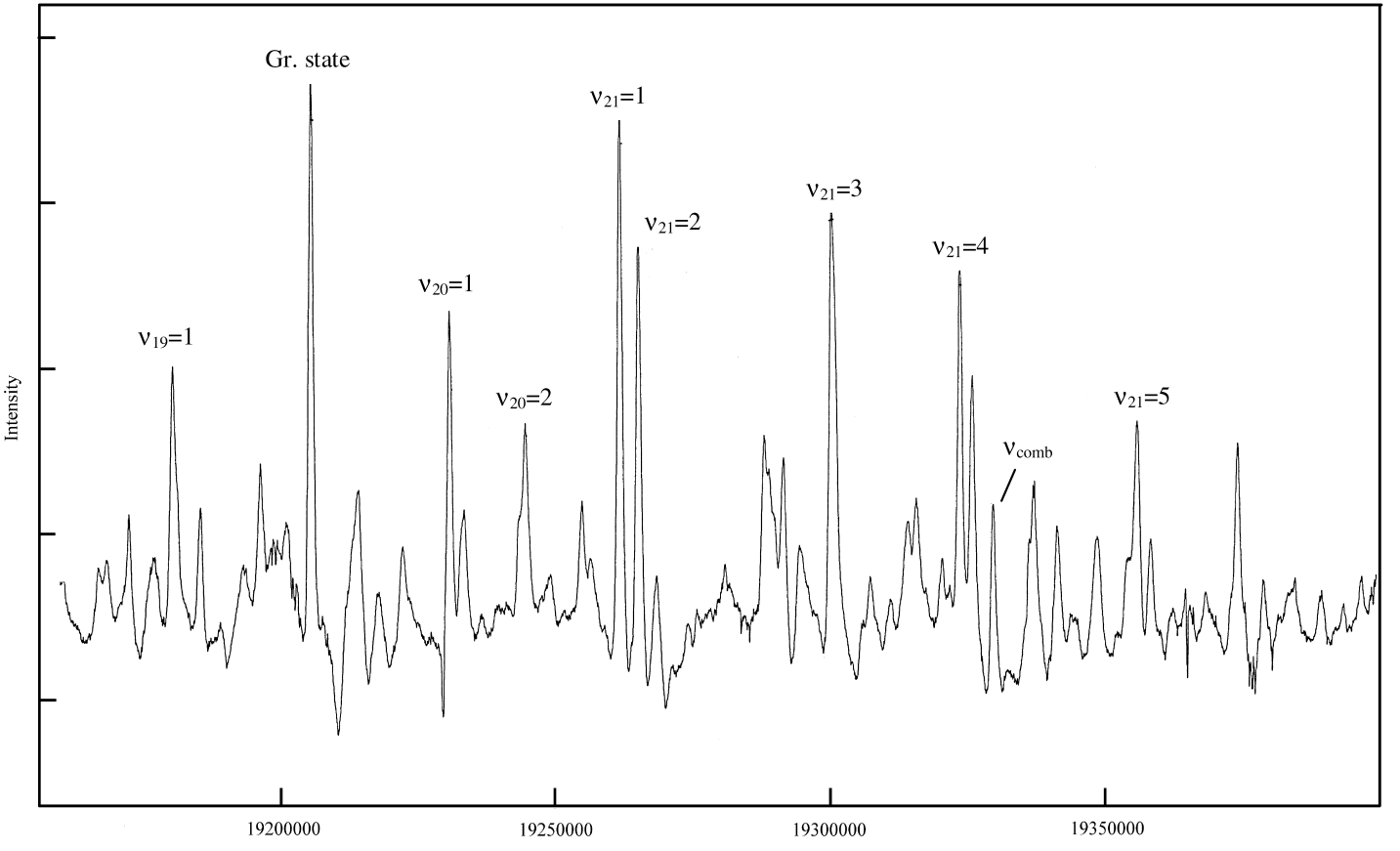

Fig. 8. The Stark spectrum of the $6_{1,6} \leftarrow 5_{1,5}$ transition taken at approximately 2000 V cm^{-1} and a temperature of 194 K showing the complex structure of the vibrational excited states (see text).

The second most intense transition ($\nu_{21} = 2$ in Fig. 8) has approximately 80% of the intensity of the ground vibrational state at the same temperature. This corresponds to a vibrational energy of 27(10) cm^{-1}. The MP2 value for the second lowest vibrational mode, identified as the C1–O2 torsional fundamental mode, is 94 cm^{-1} and the B3LYP value is 91 cm^{-1}. It is therefore, assumed that the excited state, which is 27(10) cm^{-1} higher in energy than the ground vibrational state, is the second excited state of the C3–O2 torsional vibration rather than the first excited state of the C1–O2 torsion.

The third excited state ($\nu_{21} = 3$) of the O2–C3 torsion is 60(15), the fourth ($\nu_{21} = 4$) is 88(20), and the fifth ($\nu_{21} = 5$) 142(20) cm^{-1} above the ground state (see also Table 4).

The first excited state of the C1–O2 torsional mode ($\nu_{20} = 1$ in Fig. 8) was found to have an energy of 83(20) cm^{-1} in good agreement with the quantum chemical predictions (MP2: 94 cm^{-1}; B3LYP: 91 cm^{-1}) and the gas-phase IR frequency of 84 cm^{-1} (see above). A tentative assignment of the second excited state ($\nu_{20} = 2$) of this mode has also been made.

The first excited state of what is assumed to be the lowest bending mode ($\nu_{19} = 1$) was assigned and its energy is ca. 160 cm^{-1}. The B3LYP value is 210 cm^{-1} and this mode was assigned to the very weak absorption band at 215 cm^{-1}, Fig. 4.

No definite assignment can be offered for the excited state denoted $\nu_{comb.}$ in Fig. 8. Its frequency is ca. 200 cm^{-1}. This excited state is probably a combination level.

3.4. Barrier to planarity for the H6–C1–O2–C3–H9 chain of atoms

A near-harmonic O2–C3 torsional vibration would have produced an almost equidistant frequency spacing between successive vibrationally excited states for each rotational transition, and the intensities of the vibrational excited state lines would have decreased exponentially. However, such behaviour was not observed, as seen in Fig. 8. The excited states form an irregular pattern, as seen in the same figure. This would be typical for a molecule possessing a double minimum potential with a low barrier height. The MP2 computations (see above) indicate that such a potential exists. The maximum is found when the H6–C1–O2–C3–H9 link of atoms lies in one plane.

A simple quantitative treatment has been made as follows: it is assumed that the O2–C3 torsion has a double minimum potential. According to Gwinn and co-workers [28,29], it is possible to define a potential function for the torsion of the form

$$V = V_4(\langle z^4\rangle + V_2/V_4\langle z^2\rangle) \quad (1)$$

where z is a dimensionless co-ordinate. If V_2 is *positive*, the H6–C1–O2–C3–H9 chain of atoms would lie in one plane in its equilibrium conformation; and if V_2 were *negative* a potential hump exists at this conformation and the potential function would be of the double-minimum type.

The Gwinn theory [28,29] implies that rotational constants can be expanded in a power series of the expectation values of z^2 and z^4,

$$B_n = b_0 + b_2\langle z^2\rangle_n + b_4\langle z^4\rangle_n \quad (2)$$

where B_n is the rotational constant in the nth excited state of the torsional mode. b_0, b_2 and b_4 are empirical parameters adjusted to give the best fit to the data. The values of $\langle z^2\rangle_n$ and $\langle z^4\rangle_n$ depend only on the value of V_2/V_4 in Eq. (1).

The rotational constants of successively excited states of the torsional vibration were fitted by the least squares to Eq. (2) employing the computer programs described in Ref. [30] for a series of values of V_2/V_4. It was found that the value $V_2/V_4 = -2.9$ yielded the best overall fit (Table 5). This negative value of V_2/V_4 is thus evidence that the AS conformer indeed has a double minimum for the C2–O3 torsion.

The fit is not perfect especially for the *A* rotational constants, as seen in Table 5. Such discrepancies are to be expected when a simple one-dimensional model like the one in Eq. (1) is utilised for fitting when interaction with other vibrational modes, e.g. the C1–O2 torsion, is likely to occur, as is presumed to be the case here.

The V_4 constant (Eq. (1)) was then adjusted to reproduce the torsional frequencies shown in Table 6. This was achieved with $V_4 = 9.0$ cm^{-1}. The potential function derived in this manner is $V = 9.0$ $(\langle z^4\rangle - 2.9\langle z^2\rangle)$ cm^{-1}. It is sketched in Fig. 9 and presumed to give a semi-quantitative description of the potential function near the bottom of the C2–O3

Table 5
Comparison of calculated and observed rotational constants (MHz) for the $\nu_{21} = 0$–5 states using $V_2/V_4 = -2.9$

ν_{21}	A_n[a]	Calculated − observed[b]	B_n[a]	Calculated − observed[b]	C_n[a]	Calculated − observed[b]
0	4631.118	−0.032	1913.122	0.130	1524.174	0.046
1	4647.794	−0.486	1914.183	0.185	1529.282	0.061
2	4649.470	−0.490	1911.921	−0.057	1529.814	−0.217
3	4662.063	1.014	1911.151	0.576	1533.684	−0.009
4	4672.048	2.758	1908.534	−0.616	1536.768	0.524
5	4680.785	−2.205	1907.250	0.351	1539.458	−0.330

Calculated rotational constants (MHz)
$A_n = 4607.9(68) + 24.8(87)\langle z^2\rangle_n + 1.4(16)\,\langle z^4\rangle_n$
$B_n = 1910.1(17) + 7.1(22)\langle z^2\rangle_n - 2.08(40)\langle z^2\rangle_n$
$C_n = 1517.1(12) + 7.5(15)\langle z^2\rangle_n + 0.46(28)\langle z^4\rangle_n$

[a] Calculated rotational constants using the $\nu_{21} = 0$ through $\nu_{21} = 5$ torsional states; see text.
[b] Observed: experimental rotational constants listed in Table 4.

torsional potential. A barrier height of 19 cm^{-1} for a co-planar arrangement for the H6–C1–O2–C3–H9 link of atoms is calculated from this potential. The MP2 value was lower (3 cm^{-1}). A fit using the latter value for the barrier height and $V_2/V_4 = -2.9$ predicted values for the torsional frequencies, which were much too low.

The fundamental C2–O3 torsional vibrational frequency calculated with this potential is 9 cm^{-1}. Hot bands occur at 27, 29, 34, 37, 41, 43, 46 cm^{-1}, etc. A weak absorption band observed in the IR spectrum around 34 cm^{-1} (Fig. 4) is consistent with this potential.

3.5. Dipole moment of antiperiplanar–synperiplanar

The dipole moment was determined in the standard way [31]. The results are shown in Table 7 and compared to the previous results [6]. The obtained values agree reasonably well, although there is some discrepancy between the μ_b component. We offer no explanation for this as the *M*-components used in the analysis of Suenram et al. [7] is not available. However, the ab initio results (Table 1) clearly indicate that the μ_b moment is quite large.

Table 6
Comparison of observed and calculated energies of excited states of ν_{21} using $V_4 = 9.0$ cm^{-1} and $V_2/V_4 = -2.9$

ν_{21}	Observed (cm^{-1})	Calculated (cm^{-1})
1	15(10)	9
2	27(10)	36
3	60(15)	65
4	88(20)	99
5	142(20)	137

The MP2 value (Table 1) for the total dipole moment is 6.01×10^{-30} C m, which is 23% high in comparison with the Stark splitting measurements (Table 7). The B3LYP value 5.17 (same units) is quite close to the observations. This shows that the MP2/6-311++G^{**} procedure designed to give good energy values and structures at a reasonable cost, may lead to comparatively poor predictions of electric properties. The cost-effective B3LYP computations yield a more reliable dipole moment than the MP2 calculations.

Dielectric constant measurements of the vapour carried out at seven temperatures in the range 305–415 K yielded 5.801(7) at 309.2 K and $6.138(3) \times 10^{-30}$ C m at 410.1 K [4]. Assuming only two conformers to be present in the vapour in significant amounts, dipole moments of $4.00(20) \times 10^{-30}$ and $9.44(13) \times 10^{-30}$ C m were derived for these conformers, respectively. Further, an energy difference between the conformers of 12.5(8) kJ mol^{-1} was estimated [4]. There is no question as to the quality and reliability of the dielectric constant measurements. However, the analysis is clearly inadequate.

3.6. Searches for antiperiplanar–antiperiplanar and synclinal–synclinal

Meyer and Morrison [4] concluded from their

Table 7
Stark coefficients and dipole moment (uncertainties represent one standard deviation. 1 Debye = 3.33564×10^{-30} C m).of anticlinal–synclinal of bis(difluoromethyl) ether, E134

Transition	$\|M\|$	$\Delta\nu E^{-2}$ (10^{-6} MHz V^{-2} cm^2	
		Observed	Calculated
$5_{1,5} \leftarrow 4_{1,4}$	0	−0.569(10)	−0.575
	2	1.11(3)	1.10
	3	3.36(10)	3.18
$6_{1,6} \leftarrow 5_{1,5}$	3	1.35(3)	1.22
	4	2.39(5)	2.57
$4_{0,4} \leftarrow 3_{0,3}$	0	1.02(2)	1.00
	1	−0.399(7)	−0.399
	2	1.47(2)	1.40
	3	3.93(8)	4.41
Dipole moment (10^{-30} C m)			
$\mu_a = 4.803(74)$	$\mu_b = 0.61(11)$	$\mu_c = 0.677(68)$	$\mu_{tot.} = 4.888(87)$
$\mu_a = 5.020(7)$[a]	$\mu_b = 0.19(4)$[a]	$\mu_c = 0.48(2)$[a]	$\mu_{tot} = 5.047(10)$[a]

[a] From Ref. [7].

dipole-moment determination that there is more than one conformer in the gas phase because the dipole moment showed temperature dependence. Our infrared and Raman studies also suggest the existence of more than one conformer present in the vapour.

Extensive searches have been made in the MW spectrum for AA and GG. Both these rotamers are predicted to have substantial dipole moments (Table 1). If the energy differences shown in the same table are correct, then there would be roughly 5% of GG and 1% of AA in the gas phase at 195 K.

There are several weak transitions in the spectrum that have not been assigned. These transitions could belong to a second form, or to impurities. That they are high-*J*b- or c-type transitions belonging to AS is also a possibility. Attempts to assign them have, however, failed. It is concluded that any further rotameric forms of E134 than AS are present in small concentrations, presumably less than 10% of the total at 194 K. AS is undoubtedly the preferred form of the molecule in all phases.

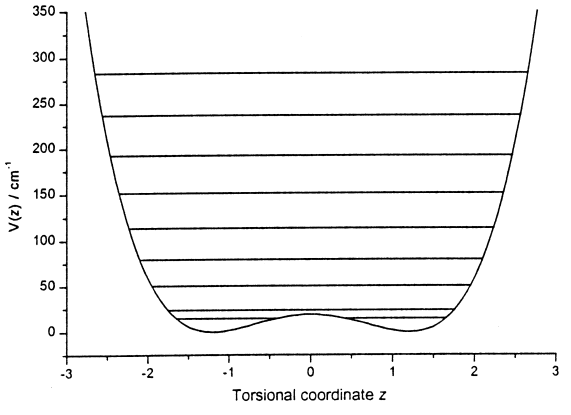

Fig. 9. The potential energy function $V = 9.0\,(\langle z^4\rangle - 2.9\langle z^2\rangle)$ cm^{-1} and energy levels.

3.7. Structure

The observed and theoretical rotational constants of AS agree to within 0.9% for the A_0, 0.1% for B_0 and 0.2% for C_0 rotational constants. If we consider the rotational constants corrected for the large amplitude torsional motion in ν_{21}, the agreement in all cases is better than 0.4%. The MP2/6-311++G** structure (Table 1) is therefore suggested as a more plausible structure for AS than the mixed theoretical/experimental r_0-structure presented by Suenram et al. [7].

Acknowledgements

This work has received support from The Research Council of Norway (Programme for Supercomputing) through a grant of computer time and from the Environment Programme of the University of Oslo.

References

[1] W.L. Kopko, Int. J. Refrig. 13 (1990) 79.
[2] C.W. Meyer, G. Morrison, J. Chem. Engng. Data 36 (1991) 409.
[3] K.A. Gillis, Int. J. Thermophys. 15 (1994) 821.
[4] C.W. Meyer, G. Morrison, J. Chem. Engng. Data 36 (1991) 409.
[5] D.R. Defibaugh, K.A. Gillis, M.R. Moldover, G. Morrison, J.W. Schmidt, Fluid Phase Equilib. 81 (1992) 285.
[6] R.A. Buono, R.J. Zauhar, C.A. Venanzi, J. Mol. Struct. (Theochem) 370 (1996) 97.
[7] R.D. Suenram, F.J. Lovas, A.R. Hight Walker, D.A. Dixon, J. Mol. Spectrosc. 192 (1998) 441.
[8] R. Imasu, A. Suga, T. Matsuno, J. Met. Soc. Jpn. 73 (1995) 1123.
[9] A.E. Heathfield, C. Anastasi, A. McCulloch, F.M. Nicolaisen, Atmos. Environ. 32 (1998) 2825.
[10] G. Myhre, C.J. Nielsen, D.L. Powell, F. Stordal, Atmos. Environ. (1999) in press.
[11] P. Basu, T.H. Ballinger Jr., J.T. Yates Jr., Langmuir 5 (1989) 502.
[12] M.-L.H. Jeng, B.S. Ault, J. Mol. Struct. 246 (1991) 33.
[13] F. Cavalli, M.D. Hurley, J. Hjorth, B. Rindone, N.R. Jensen, Atmos. Environ. 32 (1998).
[14] S. Radice, M. Causa, G. Marchionni, J. Fluorine Chem. 88 (1998) 127.
[15] Z. Zhang, R.D. Saini, M.J. Kurylo, R.E. Huie, J. Phys. Chem. 96 (1992) 9301.
[16] N.L. Garland, L.J. Medhurst, H.H. Nelson, J. Geophys. Res. 98 (1993) 23107.
[17] K.-J. Hsu, W.B. DeMore, J. Phys. Chem. 99 (1995) 11141.
[18] G.A. Guirgis, K.-M. Marstokk, H. Møllendal, Acta Chem. Scand. 45 (1991) 482.
[19] Ø. Waal, private communication, 1994.
[20] F.A. Miller, B.M. Harney, Appl. Spectrosc. 28 (1968) 350.
[21] M.J. Frisch, G.W. Trucks, H.B. Schlegel, P.M.W. Gill, B.G. Johnson, M.A. Robb, J.R. Cheeseman, T. Keith, G.A. Petersson, J.A. Montgomery, K. Raghavachari, M.A. Al-Laham, V.G. Zakrzewski, J.V. Ortiz, J.B. Foresman, C.Y. Peng, P.Y. Ayala, W. Chen, M.W. Wong, J.L. Andres, E.S. Replogle, R. Gomperts, R.L. Martin, D.J. Fox, J.S. Binkley, D.J. Defrees, J. Baker, J.P. Stewart, M. Head-Gordon, C. Gonzalez, J.A. Pople, GAUSSIAN 94, Revision B.3, Inc., Pittsburgh PA, 1995.
[22] C. Møller, M.S. Plesset, Phys. Rev. 46 (1934) 618.
[23] K.-M. Marstokk, H. Møllendal, Acta Chem. Scand. 52 (1998) 296.
[24] A.D. Becke, J. Chem. Phys. 98 (1993) 5648.
[25] P. Pulay, G. Fogarasi, G. Pongor, J.E. Boggs, A. Vargha, J. Am. Chem. Soc. 105 (1983) 7037.
[26] J.K.G. Watson, in: J.R. Durig (Ed.), Vibrational Spectra and Structure, 6, Elsevier, Amsterdam, 1977, p. 1.
[27] A.S. Esbitt, E.B. Wilson, Rev. Sci. Instrum. 34 (1963) 901.
[28] W.D. Gwinn, A.S. Gaylord, International Review of Science, Series Two, Butterworth, London, 1976, p. 205.
[29] A.C. Legon, Chem. Rev. 80 (1980) 231.
[30] K.-M. Marstokk, H. Møllendal, S. Samdal, E. Uggerud, Acta Chem. Scand. 43 (1989) 351.
[31] K.-M. Marstokk, H. Møllendal, Acta Chem. Scand. Ser. A 36 (1982) 517.